

QoS scheme for multimedia multicast communications over wireless mesh networks

M. Iqbal¹ X. Wang² S. Li² T. Ellis¹

¹Faculty of Computing, Information Systems and Mathematics, Kingston University, Kingston upon Thames, Surrey KT1 2EE, UK

²School of Engineering, Swansea University, Swansea, UK
E-mail: m.iqbal@wirelesslive.net

Abstract: A quality of service (QoS) scheme for multimedia multicast communications in wireless mesh networks (WMNs) is proposed in this study. It uses a new bandwidth calculation scheme to provide rate-adaptive admission control. It relies on information it receives from the network and application layers to calculate the network bandwidth consumption and operates independently of the media access control (MAC) layer. Using the proposed QoS scheme, the network layer provides feedback on network congestion to the application layer. The multimedia multicast sender adapts the real-time data transmission rate based on the network congestion feedback it receives. In this study, the authors describe the detailed architecture of the proposed QoS scheme. Furthermore, the authors have implemented the QoS scheme in our previously developed uni-directional link aware multicast extension to AODV (UDL-MAODV) routing protocol. The authors present validation tests to ensure the correct functionality of the QoS algorithm using our SwanMesh WMN testbed. The authors have also performed simulation tests to evaluate the performance of the proposed scheme. The simulation results show the effectiveness of the proposed QoS scheme.

1 Introduction

Wireless communications are widely used to provide ubiquitous multimedia and best-effort services. As opposed to the wired networks, wireless communications allow people to access these services anytime and anywhere. Most widely used access networks that facilitate such services are wireless local area networks (WLAN) [1], mobile *ad hoc* networks (MANETs) [2] and wireless mesh networks (WMNs) [3]. WLANs are centralised networks but the coverage of WLAN technology is limited. One access point can only cover a few hundred metres. This limitation hinders the application of WLAN in large areas. On the other hand MANET consists of multi-hop self-organised router nodes that support its applications to cover a larger area. MANETs are distributed networks that do not provide a centralised control. The WMN technology is the combination of WLAN and MANET. Thus, it takes the advantages from both networks that make it a more suitable technology to provide real-time multimedia and best-effort services to cover larger areas with centralised control.

The typical infrastructure of a WMN is illustrated in Fig. 1 WMN consists of wireless mesh routers and clients. Wireless mesh routers extend the coverage and form the mesh network backhaul. Fig. 1 shows a dual radio WMN where one radio is used to serve the clients and second creates the backhaul for the network. Wireless mesh routers may use a single radio to serve the clients and provide the mesh backhaul. The wireless mesh routers not only form a network with self-organised, self-managed, self-healing connectivity but also have the capability to function as gateway nodes. The wireless mesh gateway nodes are linked to the external network to provide Internet services and integration with other networks.

Unlike MANET, mobility is not a major issue while providing networking among wireless mesh router nodes as mesh router nodes are either fixed or have a very low mobility in WMNs. Wireless mesh clients may be mobile and may form a client meshing to provide peer-to-peer networking between client devices. A hybrid WMN is a combination of client meshing and infrastructure WMNs where mesh clients can access the network through wireless

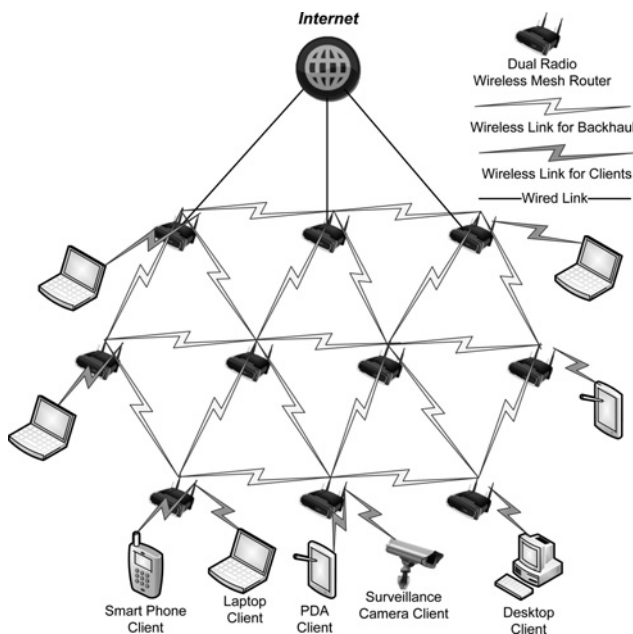


Figure 1 Architecture of WMN

mesh routers as well as directly meshing with other mesh clients [3].

The motivation for providing a rate-adaptive admission control QoS scheme for multimedia multicast traffic in our WMN [4–7] arises from WMN applications in areas such as emergency and disaster recovery [4] and healthcare [5–7] which require reliable and efficient multimedia group communications. Multimedia communications have strict QoS requirements compared to the best-effort data applications such as email, www and ftp, where packet delay and jitter have a lower impact. Facilitating the QoS requirements to provide admission control for the multimedia traffic in the presence of data traffic becomes very challenging over a wireless network because of the limited bandwidth. Most of the protocols strictly operate within their own layer. In order to provide the required QoS guarantees a cross-layer protocol design is needed, which involves the cooperation of different layers. Optimisation at a particular single layer may produce non-intuitive side effects which could result in degrading the overall system performance. In addition to the single layer restriction, the shared nature of wireless channels makes resource allocation even harder as at each mesh node the available resources are shared by all the neighbours within the carrier-sensing range. The carrier-sensing nodes are outside each other's transmission range and therefore cannot communicate directly, but still may contend for the resources.

The calculation of available sources on the network is the core of any QoS algorithm presented in recent years. Several bandwidth estimation techniques proposed over the past few years rely on the underlying MAC layer protocols to calculate the available bandwidth: Ahn *et al.* [8] use feedback from the MAC layer to perform bandwidth

estimation; Chen and Ko [9] use code division multiple access (CDMA)/time division multiple access (TDMA) for channel access at the MAC layer, which is a multicast protocol; Yang and Kravets [10] use passive monitoring of the channel at the MAC layer within carrier-sensing range; EARA-QoS [11] also depends on the MAC layer to provide QoS; Vo and Hong [12] use free and busy time monitoring of channels at the MAC layer and then piggybacks the information onto 'hello' messages to update the neighbours; Chen and Heinzelman [13] also listen to the channel to estimate the bandwidth consumption on a node based on free and busy time monitoring and uses 'hello' messages to inform two hop neighbours.

Surveys presented in [14, 15] have discussed most major contributions to the pool of QoS routing solutions for MANETs and have classified them based on their interaction between the network and MAC layer. Hanzo and Tafazolli [15] present a classification based on the MAC protocol dependence of 20 different QoS routing solution proposals. The classification of QoS protocols is described in three main categories. Firstly, those protocols that require a contention-free MAC solution such as TDMA. Secondly, protocols that rely on a contended MAC protocol. Thirdly, protocols that do not depend on the MAC layer to provide QoS.

Calculating the accurate bandwidth consumption based on the MAC layer is still a challenging problem because available resources to a node are not local concepts. Bandwidth consumption at one node may affect the available bandwidth of nodes within the carrier-sensing range. However, the MAC layer-independent QoS also often comes at the cost of trade-offs such as increased complexity and extra message overhead, especially when pro-active routing is used. A reactive routing can solve these problems by discovering routes and the QoS state only when needed, thus avoiding the potential wastage of channel and energy resources. The major drawback of reactive routing is that a delay is incurred while establishing a route between source and destination nodes.

We propose a QoS scheme to provide rate-adaptive admission control. Our scheme relies on the information it receives from the network and application layers to calculate the network bandwidth consumption and works independently from the MAC layer.

In our previously developed SwanMesh [4–7] network testbed, we have used multicast communications for multimedia traffic to enable group communications over wireless networks. This not only saves network resources but also enables different clients to exchange live information wherever required.

The multicast *ad hoc* on-demand distance vector (MAODV) [16, 17] is a reactive routing protocol that creates a multicast tree from each of the sources to all

receivers to provide multicast routing. MAODV works as an extension to the *ad hoc* on-demand distance vector (AODV) [18] unicast routing protocol. Its route-discovery mechanism is based on AODV. MAODV also utilises the control messages that exist in AODV and employs the same route request and route reply discovery cycle during its multicast route-discovery operation. Thus route information obtained during multicast route-discovery operations increases unicast routing knowledge and vice versa.

SwanMesh requires multicast routing to enable its multimedia multicast operation. It uses the reactive AODV routing protocol to provide unicast routing. It is important that the traditional on-demand view of the network routing should not be compromised while providing multicast routes. Therefore we have developed an implementation to multicast extension to AODV (MAODV) in the Linux Kernel 2.6 user space, which we call uni-directional link aware MAODV (UDL-MAODV).

MAODV forms a bi-directional shared tree for its multicast data transmission and does not support multicast over unidirectional links. MAODV assumes that the links are bidirectional, but in the presence of unidirectional links even networks of two nodes cannot survive. Therefore sensing and avoiding unidirectional links is crucial for the reliability of multicast transmission of multimedia applications over WMNs. We have proposed modifications to the MAODV basic draft to introduce a uni-directional link detection (UDL) process during our implementation. The proposed UDL process is integrated into MAODV to improve its reliability during route discovery by detecting and avoiding unreliable and unidirectional links. Thus these modifications enable UDL-MAODV to ensure a reliable route establishment during multimedia multicast communication over WMNs in the presence of unidirectional links. The process is only invoked during the multicast operation, thus this approach minimises the operating overheads by invoking the process in an on demand fashion. Furthermore, we have integrated the UDL handshaking process into the MAODV route request–route reply cycle in such a way that it does not cause any delay during the cycle at forwarding nodes. Only at a destination node is the route request–route reply cycle affected by the UDL handshaking.

The remainder of this paper is organised as follows: Section 2.1 describes the design of the proposed QoS scheme; in Section 2.2 we present our new bandwidth calculation scheme; Section 2.3 describes the detailed architecture of our QoS enabled UDL-MAODV implementation. We present validation tests in Section 3.1 using our SwanMesh testbed to ensure the correct functionality of our implementation. We present simulation test results in Section 3.2 for the performance evaluation of the proposed QoS scheme. In Section 4 we present our conclusions.

2 QoS scheme for multimedia communications over WMN

In this section we describe the detailed architecture of our QoS scheme.

2.1 QoS scheme architecture

We propose a new QoS scheme as shown in Fig. 2 for WMNs. It satisfies the critical QoS requirements of the real-time applications in the presence of best-effort traffic, by providing a rate-adaptive admission control scheme for multimedia multicast traffic.

Multimedia real-time applications use multicast communication to provide group communications. The UDL-MAODV provides multicast routing to support multicast functionality in our SwanMesh. Best-effort applications mostly use unicast communications to exchange information between WMN mesh clients and external networks via gateway nodes. AODV does not provide multiple gateway support and therefore we have designed and implemented a load balanced gateway discovery algorithm which we refer to as LBGD-AODV [5]. It provides multiple gateway support with load balancing in our SwanMesh to facilitate best-effort data applications. When a mesh router needs to communicate to the external network, LBGD-AODV selects an appropriate gateway with an appropriate route. Thus it not only provides multiple gateway support but also helps to balance the load among all gateway nodes and avoid congestion on a single route. Apart from the LBGD-AODV congestion avoidance algorithm, the unicast traffic also enjoys the advantage of using reliable transmission control protocol (TCP). TCP has its own congestion control mechanism [19] while multimedia traffic uses user datagram protocol (UDP) which, unlike TCP, does not detect network congestion. Therefore our QoS scheme provides the rate-adaptive admission control to multimedia multicast UDP traffic.

In order to provide QoS to the multimedia real-time traffic in the presence of best-effort unicast traffic, the proposed rate-adaptive admission control QoS scheme depends on the interaction among UDL-MAODV, LBGD-AODV and the rate-adaptive real-time video applications. The QoS scheme takes advantage of the co-operation among routing protocols at the network layer to calculate the bandwidth consumption of each node and provides congestion feedback to the application layer. To optimise the network resources, the multimedia multicast sender application adapts its sender's bit rate for the real-time traffic flows based on the network congestion feedback. H.264/MPEG-4 SVC video streaming standards can provide such rate-adaptive application functionalities [20].

The proposed rate-adaptive admission control scheme also provides strategies to support efficient priorities based on the

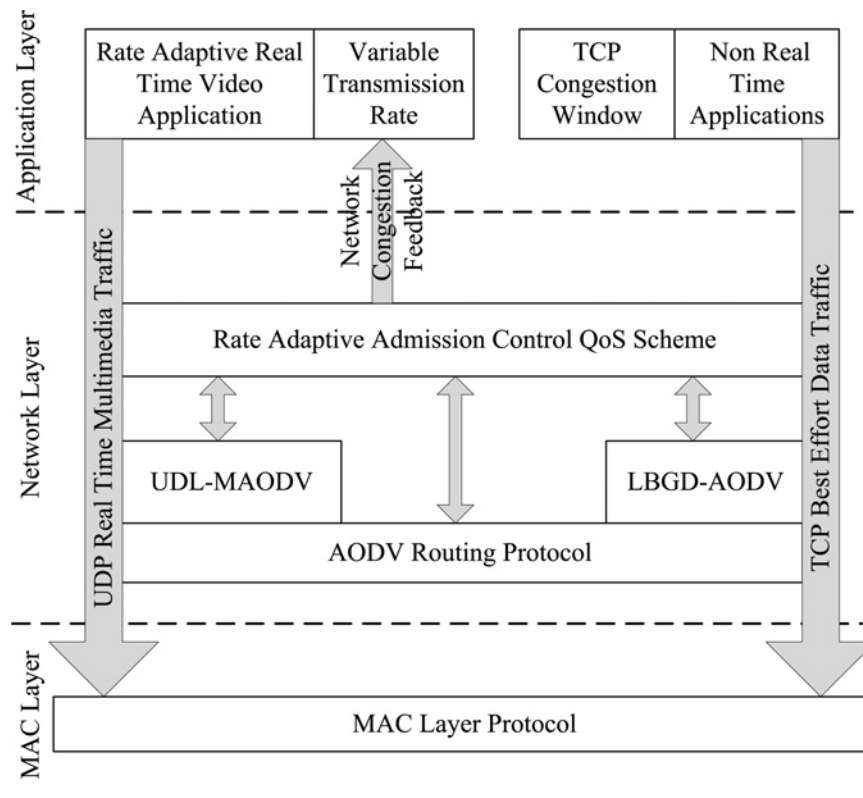


Figure 2 Architecture of QoS scheme

data flow classifications. We have classified multicast multimedia data flows as critical and non-critical. For example, an ideal application of SwanMesh is likely to be in emergency and disaster recovery. During large-scale disasters many rescue teams have to work simultaneously at different disaster affected geographical locations. SwanMesh could provide the first response and provides rescue teams with a means to exchange the crucial live multimedia information from one source camera to multiple rescue team clients to keep them informed and up to date. If a medical consultant initiates a multicast multimedia transmission for surveillance, this would be considered as non-critical because existence of such transmission is not critical to the rescue operation; therefore it may be terminated if required to free network resources for more critical operations. If the medical consultant initiates a multimedia flow to provide medical consultancy to a remote location via video conferencing during an emergency or disaster recovery operation, this may be important to save lives; therefore it is considered as critical. Critical route requests are given a higher priority while providing rate-adaptive admission control during route-discovery process.

2.2 Bandwidth calculation scheme

We propose a bandwidth calculation scheme which is similar to that as used in [21]. The scheme in [21] was proposed for unicast bandwidth consumption calculations, which was later used by Hu [22] and Darehshoorzadeh *et al.* [23] for

multicast flow bandwidth calculations. The bandwidth calculation schemes used in [21–23] depend on the MAC layer and do not consider the carrier-sensing range neighbour transmission effects while calculating the available bandwidth. It also assumes the sender rate to be known in advance. Our proposed bandwidth scheme uses a different approach. It depends on the network layer and considers carrier-sensing neighbour transmission effects while calculating a node's local bandwidth consumption. Our scheme does not assume the sender rate to be known instead it calculates the maximum bit rate that the wireless channel can support for a new flow and then provides feedback to the application layer. We modified the original work of [21] to adapt our approach and add carrier-sensing range effects. The carrier-sensing range is twice the transmission range, based on the settings of the 914 MHz Lucent Wave LAN card [13]. Owing to the carrier-sensing range effects, our proposed bandwidth calculation scheme determines the residual bandwidth within the two-hop neighbourhood range. The multicast multimedia application has predefined quality levels such as Q1, Q2, Q3, Q4 and Q5. Q1 is the quality level with the highest bit rate whereas Q5 is the quality level with the lowest bit rate. The multimedia application selects the appropriate quality level for the multicast flow so that it generates packets according to the network congestion feedback information it received.

We also used the concept for reserved bandwidth ($B_{Reserved}$) which is the bandwidth reserved for unicast data transmissions

to save them from starvation. We treat non-critical real-time multimedia flows and best-effort Internet data traffic on the same priority level. The best-effort Internet traffic uses TCP which has its own congestion control mechanism to adapt its congestion window according to the congestion level whereas multimedia UDP transmission lacks such a mechanism and generates heavy traffic load compared to Internet traffic. Therefore $B_{Reserved}$ is used to avoid unicast best-effort data traffic being starved of network resources because of unfair bandwidth consumption of non-critical multimedia flows. We limit the bandwidth use of non-critical flows by reserving bandwidth for best-effort Internet traffic. It is hard to define a partitioning scheme in order to allocate $B_{Reserved}$ for best-effort Internet traffic because best-effort Internet usage may vary from one application scenario to another, thus in our proposed QoS scheme, we keep the $B_{Reserved}$ allocation flexible to enable the user to define a $B_{Reserved}$ parameter to allocate a more suitable percentage of channels available bandwidth at the time of deployment. Considering higher traffic load and bandwidth consumption of non-critical multimedia flows by default, we set $B_{Reserved}$ to reserve 30% of channel resources for best-effort Internet traffic which is expected to be changed at the time of network deployment to define a more appropriate percentage according to the application scenario and network usage profile. Thus $B_{Reserved}$ bandwidth reservation value is based on a user assumption of required network resources for non-critical flows and best-effort Internet traffic to facilitate a fair usage of network resource. The reserved bandwidth ($B_{Reserved}$) is not guaranteed in the presence of critical multimedia flows because during the proposed QoS-enabled route discovery if non-reserved bandwidth is being fully used by other critical flows then a new critical flow will use the reserved bandwidth ($B_{Reserved}$). The available bandwidth ($B_{available}(I)$) is the available link capacity on a given node I which is calculated as follows

$$B_{available}(I) = B - B_{agg}(I) - B_{Reserved} \quad (1)$$

B is the raw data rate of a node's channel; it is usually the capacity of the link. Aggregate bandwidth $B_{agg}(I)$ is the total data traffic within node I 's carrier-sensing range neighbours. It can be calculated according to (2)

$$B_{agg}(I) = \sum_{j=1}^N B_{self}^j(I) + B_{c-neighbour}(I) \quad (2)$$

where $B_{self}^j(I)$ is a node's self-bandwidth consumption which is the total amount of data traffic transmitted by N different existing flows J at node I . $B_{c-neighbour}(I)$ is the existing active data traffic transmitted by node I 's carrier-sensing range neighbours.

Let $R_{max}(f, I)$ represent the maximum sender bit rate for a new flow f that can be supported on a given node I . Thus the multimedia application sender bit rate value is determined by the bottleneck value for $R_{max}(f, I)$ of the nodes on the route

from source to destination. Therefore we calculate $R_{max}(f, I)$ for each node on the route as follows, if it is not a destination node

$$R_{max}(f, I) = \frac{B_{available}(I)}{N_{c-sender} + 1} \quad (3)$$

in which $B_{available}(I)$ is the available bandwidth link capacity on a given node I which is calculated using (1) and $N_{c-sender}$ is the number of active sender/forwarders for a new flow f within the carrier-sensing neighbourhood of node I . If node I is a destination node then $R_{max}(f, I)$ is calculated as follows

$$R_{max}(f, I) = \frac{B_{available}(I)}{N_{c-sender}} \quad (4)$$

because the destination nodes only passively receive the data and are not active senders.

With help of example scenarios, Fig. 3 further explains how to calculate value for $N_{c-sender}$ in order to calculate $R_{max}(f, I)$.

Once we have the value for the bottleneck-rate $R_{max}(f, I)$ on the route, we send it to the multimedia sender which selects an appropriate quality level to adapt its quality and

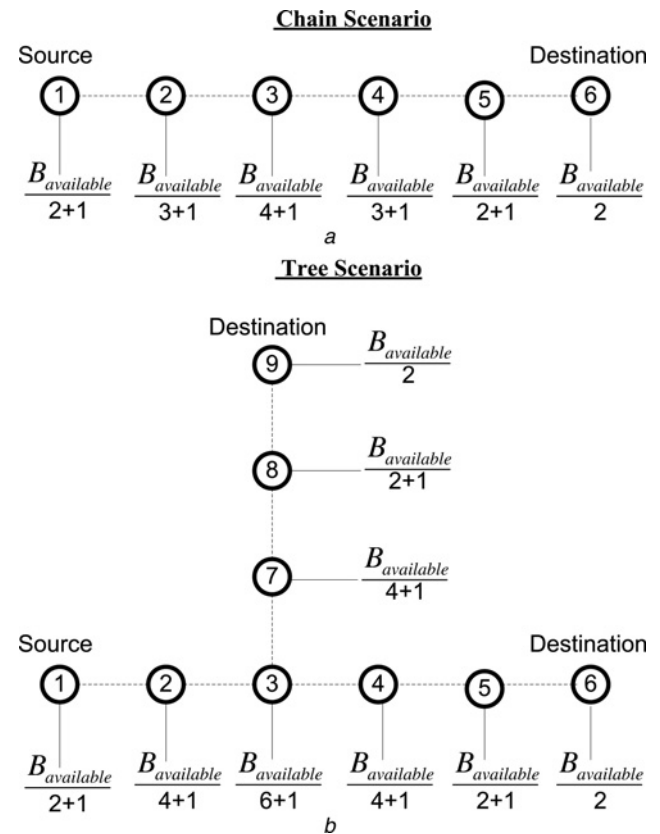


Figure 3 UDP traffic flow self interference

only generates packets at a rate no greater than the bottleneck-rate value of $R_{\max}(f, I)$ on the route.

2.3 QoS enabled UDL-MAODV architecture

During our UDL-MAODV implementation in SwanMesh, we observed that the multicast receiver rate drops and packet loss increases at each hop as the distance between sender and receiver node increases. The situation becomes worse on longer routes. This is because there are more forwarding nodes on the longer routes. As a result these nodes may contend for the wireless channel within carrier-sensing range of each other. This leaves each node on the route with a different available link capacity because of flow's self-interference which affects the bottleneck node's available bandwidth on the route. We have made some modifications to the basic architecture of MAODV [17] to improve its performance in this situation. The modifications not only enables the proposed QoS scheme during its route-discovery process but also helps maintain a minimum hop distance between the sender node and receiver nodes while forming the multicast tree. In order to implement the QoS scheme, we modified the multicast group information extension to the route reply (RREP) message to carry additional bandwidth information (BI) during route-discovery process. The extension is described in [17]. Furthermore, we have introduced a new BI message. It is used by a node to share the bandwidth consumption information with the carrier-sensing neighbours. Each node within the carrier-sensing range of the flow maintains a BI table to store the bandwidth consumption locally. This information is used to calculate the available bandwidth using the bandwidth calculation scheme described in Section 2.2. Later in this section we describe more details of the proposed modifications.

2.3.1 Modifications to the basic MAODV operations: We have modified the basic operation for MAODV to enable QoS during route discovery. Full details of the MAODV protocol operation are described in [17]. During the route-discovery process of MAODV, if a node is the first one to run a multicast application then it becomes a group leader. All the other nodes that join the group later accept the first node as their group leader. We made changes to this basic MAODV process to support our QoS scheme. During our proposed QoS-enabled route discovery the multicast sender node always becomes the group leader regardless of whether the sender node is the first one to join the group or not. If the sender node joins a group which already has a group leader, in this case as soon as the existing group leader detects the sender node it gives up its leadership. Thus all the members of the group including the old leader set the sender node as their leader. We have introduced a new flag *S* in the group hello message which indicates that the leader is a sender node. We have implemented the proposed modifications in the

operation using MAODV standard control messages and flags used during the tree merger process described in [17].

2.3.2 Modifications to the route selection criteria:

During MAODV operations when a node wishes to join a multicast group it broadcasts a RREQ (route request) with the '*J*' flag. Only nodes that are members of the multicast group can respond to the RREQ with a RREP (route reply). A non-member node will rebroadcast the RREQ packet. Regardless of whether it is the group leader or group member which generates the RREP, the RREP hop count field is always set to zero. When the intermediate node receives the RREP it increments the hop count and multicast group hop count fields and relays this packet back to the node that originated the RREQ. When the RREQ originator node receives more than one RREP for the same RREQ, it selects the route based on the one that has the greatest sequence number. In case a node receives more than one RREP with the same (largest) sequence number then it would select the route based on the RREP that has smallest hop count, that is, the shortest distance to a member of the multicast tree.

The problem with selecting a route based on smallest hop count is that it does not select a route with lower hop distance to the group leader. Owing to the modifications described in Section 2.3.1, the sender node will always be the group leader. Therefore we have modified MAODV to select a route based on the distance to the group leader instead of the distance to the group member. This will enable the selection of a route based on the shortest distance between sender and receiver nodes. Thus it will improve the performance.

2.3.3 Modifications to multicast group information extension for RREP:

The network congestion is the main route selection criteria for our QoS-enabled UDL-MAODV apart from the hop distance to the sender node. In order to incorporate QoS in the route-discovery process, we have modified the multicast group information extension to the RREP message. We modified the original extension to carry additional BI with the RREP message when RREP is sent to establish a route to the multicast destination. Fig. 4 shows the size and format of the modifications. We have added the emboldened as shown in the Fig. 4. With the proposed modifications the value of the length field is set to 12 instead of 6. The multimedia sender node does not transmit the multimedia multicast data until it has at least one multicast group receiver and the route between the sender and a receiver is established with an appropriate quality level. If the group leader (i.e. the sender node) is the only member of the group and it receives a RREQ from a node which wishes to join the group, then it generates a RREP message in response to that RREQ. Before the group leader sends the RREP it calculates and adds the value of $R_{\max}(f, I)$ to the bottleneck-rate field of RREP extension.

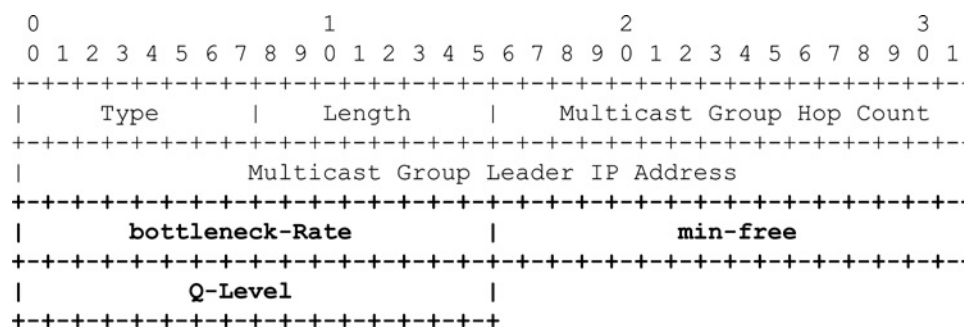


Figure 4 Modified multicast group information extension to the RREP message

The min-free field of the RREP extension is used to add information on how much additional bandwidth a node can set free by terminating the non-critical C-neighbour's (carrier-sensing neighbour) flows within its carrier-sensing range. If the multicast RREP is for a critical flow and the calculated $R_{\max}(f, D)$ value is less than Q5, then the group leader adds information to the min-free field. This is because if $R_{\max}(f, D)$ is less than Q5, it means that the group leader does not have enough available bandwidth to support the critical flow with even the minimum quality level; therefore it adds information on how much bandwidth it can set free by terminating non-crucial flows operating within its carrier-sensing range.

When an intermediate node receives that RREP, it calculates its residual $R_{\max}(f, D)$ and compares the residual $R_{\max}(f, D)$ with the bottleneck-rate field in the RREP. If its residual $R_{\max}(f, D)$ is greater than the bottleneck rate, it forwards the RREP. Otherwise, it updates the bottleneck-rate value using its residual $R_{\max}(f, D)$ before it sends it back to the originator RREQ node. If the RREP is for a new critical flow and $R_{\max}(f, D) < Q5$ then the intermediate node also makes a calculation on how much additional bandwidth it can free by terminating the non-critical flows within its C-neighbourhood. If the value is less than min-free it updates the min-free value using its calculated value of potential bandwidth that can be set free. If the value is higher than the min-free then the intermediate node does not update the min-free. Thus when the RREP reaches the originator of the RREQ, the value of min-free field indicates the maximum additional bandwidth that can be set free for the critical flow on the route from source to destination. The min-free field is not used during route discovery of non-critical flows.

The Q-level field is only used if the multicast group leader or a multicast tree member is already actively sending/forwarding/receiving a critical flow for which they have received the RREQ. In this case the group leader or group member checks the quality level of their existing critical flows for which they are generating the RREP and sets the quality level value to the Q-level field. If the value of $R_{\max}(f, D)$ on the RREP originator node or an intermediate node is less than the Q-level field then the node also updates the min-free field if required.

Non-critical flows are always transmitted using quality level Q5 because these flows are of lower priority. Q5 uses a multimedia transmission sender rate which provides the lowest but acceptable multimedia quality for these flows. Their existence is not critical to the operations provided by WMN in different application scenarios. Therefore if required an active non-critical flow may be terminated by the proposed QoS scheme to accommodate a critical flow. Transmitting these flows at lowest but acceptable quality level Q5 keeps the network congestion caused by them as low as possible at all times, thus it eventually lowers the frequency of these flows being terminated. Therefore if a RREP is generated for a non-critical flow then the Q-level information is not provided.

A node learns about the flow's priority as critical or non-critical based on its multicast group IP address. We have classified multicast group IP addresses as critical and non-critical. The range of critical multicast IP address can only be used for critical group communications.

When the RREP reaches the node which has originated the RREQ, it carries all the information a node needs to know before making a decision on route selection. The flowchart shown in Fig. 5 further explains how the information obtained from the extension of RREP is used to enable QoS during the route-discovery process.

Once the route has been found between source and destination nodes then it is activated using the existing multicast activation (MACT) message described in [17]. We introduced a new flag T . This flag is turned on if the node selects a route for a critical flow that requires all the nodes on the route to terminate non-critical flows within their C-neighbour range. We utilised reserved bits in the MACT message to add additional quality level information. If the node has enough bandwidth on the selected route without terminating any flow then it sends a MACT message with join flag set. The node unicasts this message to the selected next hop on the route, effectively activating the route. The standard MAODV route activation procedure explained in [17] is followed during this route activation process. When the intermediate/destination node receives a MACT with T flag, it first checks if its $R_{\max}(f, D)$ value supports the flow using the

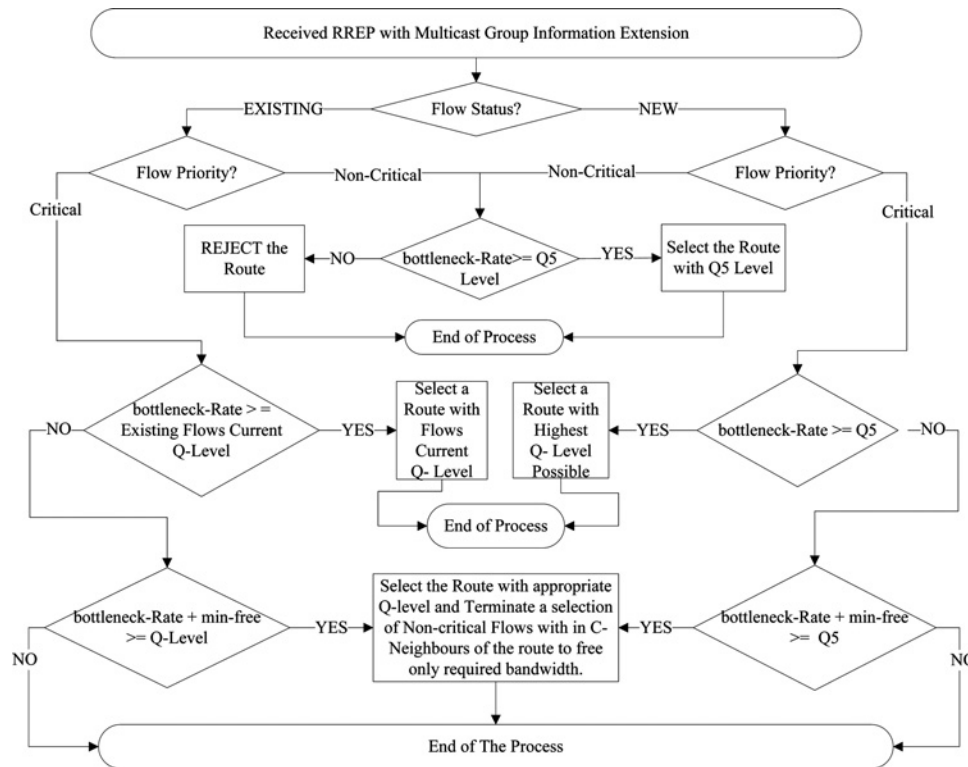


Figure 5 QoS enabled UDL-MAODV route-discovery process

requested quality level. If its available bandwidth is not enough to support the flow then the node decides how many non-critical flows should be terminated in order to accommodate the new critical multicast flow and informs the C-neighbours to terminate the selected flows. The termination of flows in C-neighbours is achieved by broadcasting a BI message which is explained in Section 2.3.4.

2.3.4 BI message: The BI control message is used to inform the two hop neighbours about the bandwidth consumption of the flow. Any node that is either sending, or forwarding the multicast data broadcasts the BI message with a TTL setting of 2. The BI message is broadcast just after a node joins the group and activates its route upon receiving a MACT message. This way a node can share its bandwidth consumption information of a particular flow with C-neighbours. The receiver nodes that are only receiving the multicast data and do not forward data are called leaf nodes. The leaf nodes do not broadcast the BI

message after joining the group. This is because leaf nodes do not consume any bandwidth while passively receiving the multicast data. Fig. 6 shows the size and format of the BI message.

When a node starts sending/forwarding a new flow, it broadcasts a BI message with the field settings as shown in Fig. 6. The flow ID indicates a unique flow number on the node. The flow rate field is used to add information on the sending/forwarding rate based on the quality level of the flow. The originator node of the BI message adds its own address in the C-neighbour IP address field. The multicast group IP address field is used to add information on the multicast group IP address of the flow. When a C-neighbour node receives a BI message, it logs all the bandwidth consumption information it carries into the BI table.

When a node leaves the multicast group it broadcasts the BI message again with the flow information and flow rate

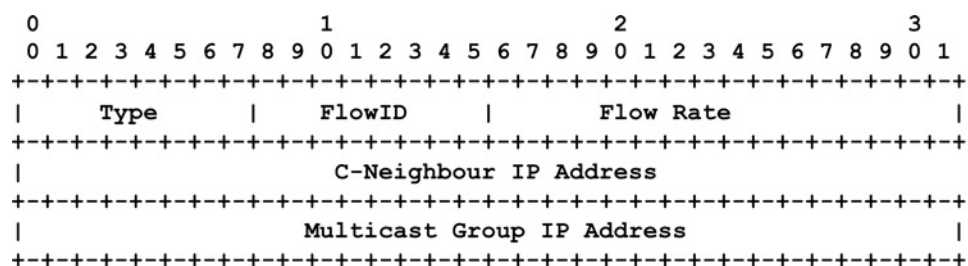


Figure 6 BI message format

set to zero. The zero flow rate value in a BI message indicates that the node has stopped sending/forwarding the flow. The TTL for broadcast is set to 2, so when a node's C-neighbours within two hops receive that flow information via BI message, they delete the flow entry from their BI table.

The BI message is also used to terminate the non-critical flows within a node's carrier-sensing range. When a node wishes to terminate selected non-critical multicast sender/forwarders to free bandwidth resources, it sends the BI message with the flow ID and flow rate both set to zero. Instead of its own address, it adds the C-neighbour node's address to which it is sending the termination request into the C-neighbour IP address field. A zero value in both fields indicates that the originator node of the BI message is requesting its selected C-neighbour to terminate the non-critical flow so that it can accommodate the critical flow. When a C-neighbour node receives the broadcast BI message with the flow ID and flow rate both set to zero, it checks the C-neighbour IP address field of the BI message. If it matches its own IP address then it terminates the group communications indicated by the multicast group IP address.

2.3.5 BI table: The BI table is used to store the information received via the BI message. Each node maintains a BI table to store the bandwidth consumption of multicast multimedia flows within the carrier-sensing range neighbourhood. The BI table has the following fields to store received information:

- flow ID,
- flow rate,
- C-neighbour IP address and
- multicast group address.

3 Validation and performance evaluation tests

3.1 Validation tests

We have implemented the QoS algorithm to enable QoS in our previously developed UDL-MAODV. To ensure the correct functionality of the implementation, we have performed the validation. We used our SwanMesh testbed to perform validation tests. Mackill (an open source MAC filter utility developed by Uppsala University in Sweden) is a utility tool which can force different connectivity configurations of mesh nodes without the nodes being required to be physically separated. We have used this utility to establish our network topology scenarios during the tests. We verified and cross-referenced the QoS-enabled UDL-MAODV operation using the multicast route table, BI table and debugging output to ensure correct functionality of our implementation. We have written several small non-multimedia sender and receiver applications in the C language to perform these validation tests.

During the validation tests we have compared the operation of both of our implementations (i.e. UDL-MAODV and QoS-enabled UDL-MAODV) using the same network topology as shown in Fig. 7. The numbered nodes show the order in which the nodes have joined the group. T stands for the members of the multicast tree nodes that are working as router nodes in order to establish the group tree between member nodes of the group (i.e. sender/receiver nodes).

During both tests as shown in Fig. 7, receiver 1 is the first one to join the group followed by receiver 2. The sender node joins the group at the end. Node 4 joined the group once nodes 1, 2 and 3 have already joined the group.

During the validation test of UDL-MAODV operation in the above scenario, when receiver 1 joins the group it becomes a group leader as it is the only member at the time. When the node 2 multicast receiver is turned on it also joins the group via T1 and T2 which becomes the members establishing a group tree between nodes 1 and 2. When the sender application is run at node 3, it joins the group via node 1 as a member. At the end we run a receiver application at node 4 which joins the group via T2 based on the lowest hop count to the next tree member. Finally, we have the UDL-MAODV multicast topology established as shown in Fig. 7.

During the validation test of the QoS-enabled UDL-MAODV operation in the above scenario, when receiver 1 joins the group it becomes a group leader as it is the only member at the time. When node 2's multicast receiver application is turned on it also joins the group via T1 and T2 which becomes the tree member in order to establish a group tree between node 1 and node 2. When the sender application is run at node 3, it joins the group as a group leader. When the node 1 group leader receives the group hello message with an S flag, it gives up its leadership for the new leader. The rest of the tree also joins the new group leader by following the standard tree merger procedure of MAODV. At the end, we run a receiver application on node 4 which joins the group leader via T3. This QoS-enabled route selection is made based on the lowest hop count to the group leader node instead of lowest hop count to the tree member. The hop count to

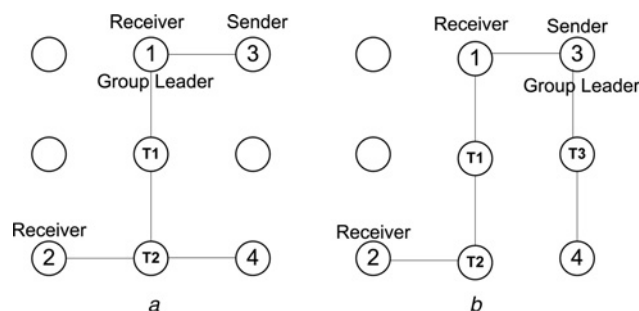


Figure 7 Validation test network topology

- a UDL-MAODV
b QoS enabled UDL-MAODV

the group leader-based route selection also needs to ensure if the available bandwidth on the selected route is enough to allow such selection. Finally, we have established a QoS-enabled UDL-MAODV topology as shown in Fig. 7.

3.2 Performance evaluation test

We have used simulation tests to evaluate the performance of our QoS scheme. Simulations were performed using the NS2 simulation tool [24]. We have used MAODV as the multicast routing protocol [25] during the simulations. NS2 considers neighbours within two hops as carrier-sensing neighbours. NS2 wireless node with the channel capacity of 2 Mbps uses a transmission range of 250 m and a carrier-sensing range of 550 m which covers a two-hop neighbour distance. The simulation environment is based on MAC 802.11b, the propagation is TwoRayGround, the PHY interface type is WirelessPhy, interface queue type is Queue/DropTail/PriQueue and queue length is 50 packets. In real-world video transmission, videos are separated into three different frames: I-frame, P-frame and B-frame. All of them are packed into UDP and sent out. During the simulations we used UDP data flow with CBR input flow type and a packet size of 512 bytes, as a substitute to the real-world video transmission. Our scheme does not depend on specific video flow and may be implemented using any scalable video coding technique. During the simulations the sender node in each flow sends multicast UDP data with the bit rate set to one of the five sender rate-based quality levels, which are defined as: $Q_1 = 250$ kbps, $Q_2 = 200$ kbps, $Q_3 = 150$ kbps, $Q_4 = 100$ kbps and $Q_5 = 50$ kbps.

The motivation behind selecting five different levels of sender bit rate is to generate different levels of congestion during several sets of simulations. In order to cover all the aspects of the network performance evaluation of our QoS scheme, we have performed 25 simulations each using three flows shown in Fig. 8. During each simulation we run three flows with different combinations of quality levels simultaneously, which

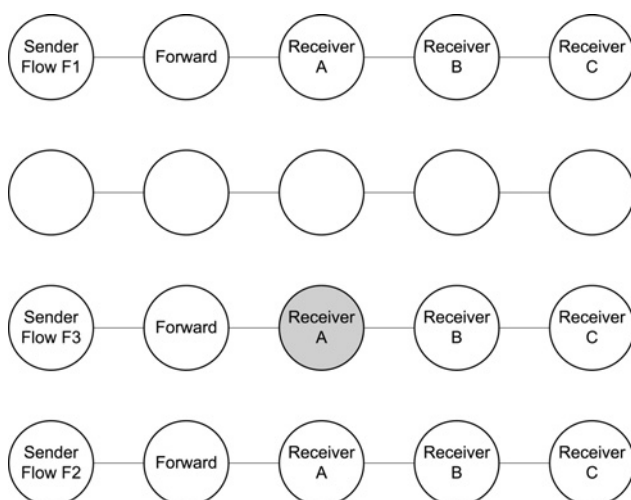


Figure 8 Simulation test topology

result in different aggregated bandwidth $B_{agg}(A)$ consumption at flow F3's Receiver A (grey shaded) node. As mentioned earlier the proposed scheme does not target a specific video application; therefore during a real implementation a user may choose more or less quality levels than five dependants on the quality layers supported by a certain scalable video coding technique and application.

As shown in the simulation topology, the flows F1 and F2 are outside each other's carrier-sensing range. Therefore the data transmission of flows F1 and F2 do not affect each other's performance, whereas flow F3 shares the bandwidth with both flows as it operates inside the carrier-sensing range of both flows F1 and F2. Therefore the data transmission of flow F3 affects the performance of the data transmission of flows F1 and F2. Similarly the data transmission of flows F1 and F2 effects the data transmission of flow F3. To study the effects of different congestion levels during each simulation, we have used different combinations of quality levels for all three flows. In order to explain, we can categorise the 25 simulations we performed into five sets. Flows F1 and F2 use multicast sender quality level Q_1 in 1st, Q_2 in 2nd, Q_3 in 3rd, Q_4 in 4th and Q_5 in 5th set. Each set contains five simulations. Flow F3 uses multicast sender quality level Q_1 in 1st, Q_2 in 2nd, Q_3 in 3rd, Q_4 in 4th and Q_5 in 5th simulation in each set. In each simulation all three flows start at the same time.

During each simulation, we recorded the packet loss results occurring at receiver C node in each flow. Figs. 9 and 10 present the simulation results. The x -axis shows the aggregated bandwidth consumption $B_{agg}(A)$ calculated using proposed bandwidth calculation scheme at flow F3's receiver A and y -axis shows the corresponding packet loss. Flow F3's receiver A node is within carrier-sensing range of both flows F1 and F2, thus it shares its channel capacity with other two flows. Since all the three flows run simultaneously, a certain flow may be consuming most of the calculated aggregated bandwidth $B_{agg}(A)$ within carrier-sensing range and enjoys lower packet loss. This would result in lower $R_{max}(f, I)$ for other flows, therefore those flows may suffer unfair packet loss. The packet loss on a wireless channel may occur because of many factors such as packet size or buffer over flow, but in this study we only focus on packet loss as a result of interference between flows within carrier-sensing range.

The aim of the simulations is to show the effectiveness of the proposed bandwidth calculation and rate-adaptive admission control QoS scheme. This is achieved with the help of results presented in Figs. 9 and 10. Fig. 9 shows different levels of aggregated bandwidth $B_{agg}(A)$ consumption calculated at flow F3's receiver A node using the proposed bandwidth calculation scheme and the effects of corresponding congestion on performance in terms of packet loss at individual flows within carrier-sensing range. As the network congestion increases the packet loss increases. This shows the effectiveness of the bandwidth calculation scheme. Fig. 10 presents further analysis of simulation results to show how

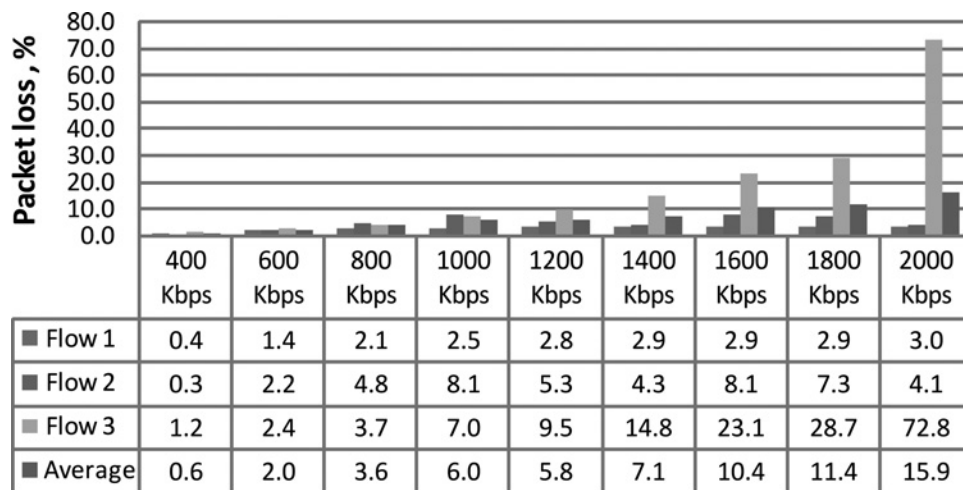
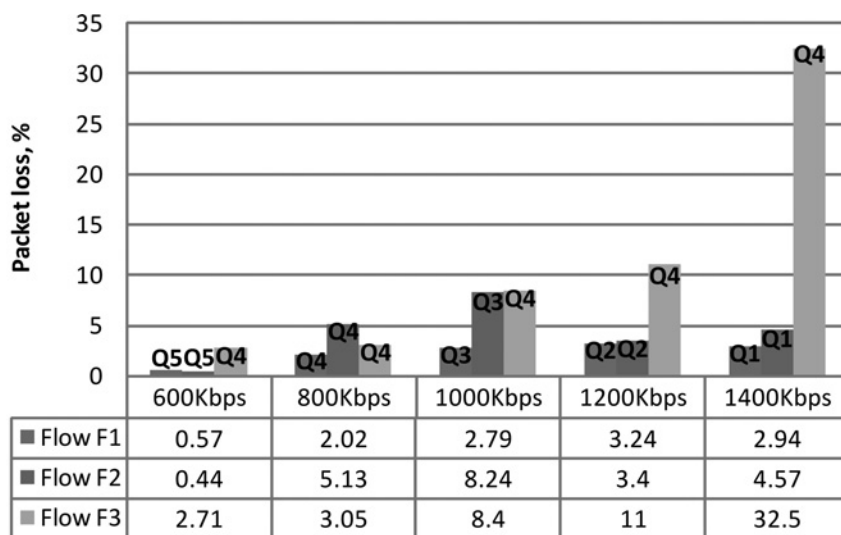
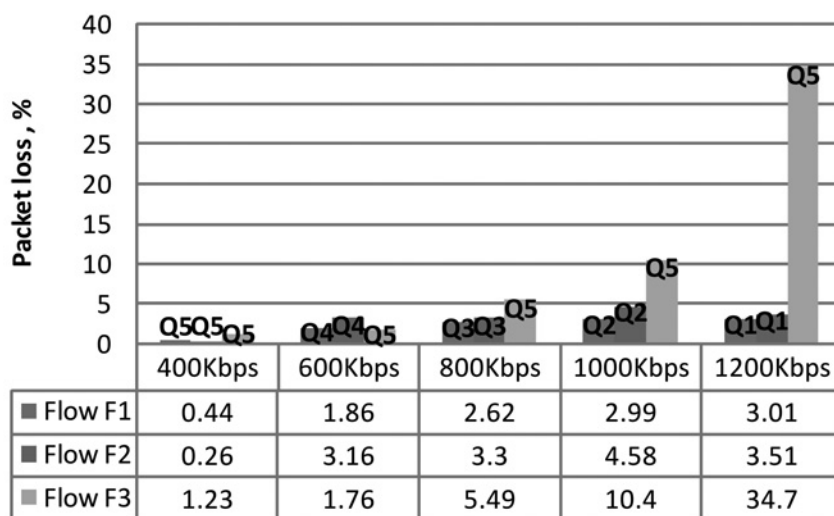


Figure 9 Network congestion based network performance analysis in terms of packet loss %



a



b

Figure 10 Network performance analysis based on flow F3 with two different quality levels

a Packet loss % for multiple flows based on flow F3 quality level Q4

b Packet loss % for multiple flows based on flow F3 quality level Q5

much performance improvement is achieved in terms of packet loss for all three flows by reducing the multicast sender quality rate of one flow by just 1 level (i.e. flow F3 from Q4 to Q5). The results show that the rate-adaptive admission control QoS scheme can improve the performance by selecting the multicast sender quality level based on network congestion within carrier-sensing range.

The graphical representation in Fig. 9 shows that during the simulations when the $B_{agg}(A)$ is calculated as 400 kbps, the corresponding packet loss on each flow is very low. The average network packet loss of the three flows is as low as 0.6%. This is because all the three flows transmit multicast data simultaneously at lowest quality level Q5. As the $B_{agg}(A)$ grows, it affects the network performance. The packet loss at each flow as well as the average network packet loss of the three flows grow higher in response to the network congestion.

During the simulations when all the three flows transmit multicast data simultaneously at highest quality level Q1, the $B_{agg}(A)$ is calculated as 2000 kbps (as shown in Fig. 9) at flow F3's receiver A. It creates huge congestion at flow F3's bottleneck node which results in 72.8% of its packets being lost for the following reasons. The wireless full channel capacity is 2000 kbps which is not fully usable because of nature of the wireless medium. Furthermore, because of shared wireless channel some flows suffer from starvation while other flows capture the most of channel usable bandwidth within carrier-sensing range. When the $B_{agg}(A)$ is calculated as 2000 kbps at flow F3's receiver A, the 1000 kbps of its usable channel capacity is being utilised by carrier-sensing range neighbour flows F1 and F2. Therefore these flows suffer comparatively low packet losses of 3 and 4.1%. Flows F1 and F2 are transmitting within flow F3's carrier-sensing neighbourhood but are outside each other's carrier-sensing range. Thus flow F3 suffers unfair packet loss. Our QoS scheme avoids such unfairness by providing rate-adaptive admission control to the flows according to flow's bottleneck congestion feedback. With the help of a graphical representation of simulation results presented in Fig. 10, we further explain how the performance has improved during the above simulations at all three flows by reducing the multicast sender quality rate of a single flow by just one level (i.e. flow F3 from Q4 to Q5).

In Fig. 10, the graph (a) represents the results in terms of packet loss of each set of simulation tests where flow F3 is using multicast sender quality level Q4. The graph also shows the corresponding aggregated bandwidth consumption $B_{agg}(A)$ at bottleneck flow F3's receiver A node during each simulation. The quality levels used by each flow during the simulation are also indicated on top of the corresponding graphical bar. Graph (b) represents the results of each set of tests where flow F3 has decreased the multicast sender quality level to Q5. The graph shows that by decreasing the multicast sender quality rate of flow F3

by just one level, the corresponding aggregated bandwidth consumption $B_{agg}(A)$ at bottleneck node of flow F3 has been reduced. Thus it has resulted in improved packet loss not only at flow F3 but has also improved the packet loss of carrier-sensing range neighbour flows F1 and F2 which are still transmitting at the same quality level.

The simulation tests show that the network performance for multicast UDP data transmission can be significantly improved using our QoS scheme. Network congestion feedback provided by the QoS scheme helps the multimedia multicast sender application to pick up the quality level that would generate packets at a rate no greater than the bottleneck available bandwidth on the route from source to destination. This would help to improve the video quality over WMNs. The simulation results of the ratio between network congestion and packet loss (both at individual flows and average network performance) shows the effectiveness of our rate-adaptive admission control and bandwidth calculation scheme.

In the future we plan to implement a rate-adaptive video application in our SwanMesh testbed to evaluate the performance of the QoS scheme and the effects of congestion feedback controls using a real application environment.

4 Conclusions

In this paper, we have described the detailed architecture of our QoS scheme and the bandwidth calculation scheme it uses. The proposed scheme provides a rate-adaptive admission control based on the network and application layers, therefore works independently of the MAC layer. Thus it can be implemented using different MAC layer standards. The multimedia multicast sender at the application layer adapts the multimedia multicast transmission's sender rate based on the network congestion feedback it receives from the network layer. We have described the detailed architecture of the proposed QoS scheme implementation in our SwanMesh WMN testbed. We have performed validation tests to ensure the correct functionality of the implemented scheme. Furthermore, to evaluate the network performance of the proposed QoS scheme, we presented simulation tests. The simulation results of the ratio between network congestion and packet loss (both at individual flows and average network performance) shows the effectiveness of our rate-adaptive admission control and bandwidth calculation scheme. The comparison of the two different quality levels used by a flow shows that by downgrading the multicast sender quality by just one level at a specific flow improved the performance of all the flows operating within carrier-sensing range, although the other flows are still transmitting at the same quality level. It shows that the network performance for multicast multimedia transmission over shared and congested wireless networks can be significantly improved using the proposed rate-adaptive admission control QoS scheme.

5 References

- [1] IEEE std. 802.11-1997: 'Wireless LAN medium access control (MAC) and physical layer (PHY) specifications', 1997
- [2] MURTHY C.S.R., MANOJ B.S.: 'Ad hoc wireless networks: architectures and protocols' (Prentice Hall, 2004, special edn.)
- [3] AKYILDIZ I.F., WANG X., WANG W.: 'Wireless mesh networks: a survey', *Comput. Netw.*, 2005, **47**, (4), pp. 445-487
- [4] IQBAL M., WANG X.H., WERTHEIM D., ZHOU X.: 'SwanMesh: a multicast enabled dual-radio wireless mesh network for emergency and disaster recovery services', *J. Commun. (Special Issue on Wirel. Commun. Emerg. Commun. Rural Wideband Services)*, 2009, **4**, (5), pp. 298-306
- [5] IQBAL M., WANG X.H., WERTHEIM D., ZHOU X.: 'Load balanced multiple gateway support in wireless mesh networks for broadband services'. Proc. 18th Wireless and Optical Communications Conf. (WOCC 09), NJIT, Newark, New Jersey, USA, 1-2 May 2009
- [6] WANG X.H., IQBAL M., ZHOU X.: 'Design and development of a dual radio wireless mesh network for healthcare'. Proc. Fifth Int. Conf. Information Technology and Applications in Biomedicine (ITAB 2008), Shenzhen, China, 30-31 May 2008, pp. 300-304
- [7] ZHOU X., WANG X.H., IQBAL M., YAN L.: 'A Handheld mobile device for wireless mesh networks in healthcare'. Proc. Second IEEE Int. Symp. on IT in Medicine & Education (ITME 2009), Jinan, China, 14-16 August 2009, pp. 1070-1073
- [8] AHN G., CAMPBELL A.T., VERES A., SUN L.: 'Supporting service differentiation for real-time and best-effort traffic in stateless wireless ad hoc networks (SWAN)', *IEEE Trans. Mob. Comput.*, 2002, **1**, (3), pp. 192-207
- [9] CHEN Y.S., KO Y.W.: 'A lantern-tree-based QoS on-demand multicast protocol for a wireless mobile ad hoc network', *IEICE Trans. Commun.*, 2004, **E87-B**, (3), pp. 717-726
- [10] YANG Y., KRAVETS R.: 'Contention-aware admission control for ad hoc networks', *IEEE Trans. Mob. Comput.*, 2005, **4**, (4), pp. 363-377
- [11] LIU Z., KWIATKOWSKA M.Z., CONSTANTINO C.: 'A biologically inspired QoS routing algorithm for mobile ad hoc networks'. Proc. Int. Conf. Advanced Information Networking and Applications (AINA'05), Taipei, Taiwan, March 2005, pp. 426-431
- [12] VO H.Q., HONG C.S.: 'Hop-count based congestion-aware multi-path routing in wireless mesh network'. Proc. Int. Conf. Information Networking (ICOIN), Busan, Korea, January 2008, pp. 1-5
- [13] CHEN L., HEINZELMAN W.B.: 'QoS-Aware routing based on bandwidth estimation for mobile ad hoc networks', *IEEE J. Sel. Areas Commun.*, 2005, **23**, (3), pp. 561-572
- [14] REDDY T.B., KARTHIGEYAN I., MANOJ B.S., MURTHY C.S.R.: 'Quality of service provisioning in ad hoc wireless networks: a survey of issues and solutions', *Ad Hoc Netw.*, 2006, **4**, (1), pp. 83-124
- [15] HANZO II L., TAFAZOLLI R.: 'A survey of QoS routing solutions for mobile ad hoc networks', *IEEE Commun. Surv. Tutorials*, 2007, **9**, (2), pp. 50-70
- [16] ROYER E.M., PERKINS C.E.: 'Multicast operation of the ad-hoc on-demand distance vector routing protocol'. Proc. Fifth Annual ACM/IEEE Int. Conf. Mobile Computing and Networking, Seattle, Washington, USA, 15-19 August 1999, pp. 207-218
- [17] ROYER E.M., PERKINS C.E.: 'Multicast ad hoc on-demand distance vector (maodv) routing'. Internet Engineering Task Force (IETF) INTERNET-DRAFT <draft-ietf-manet-aodv-00.txt>, <http://tools.ietf.org/html/draft-ietf-manet-maodv-00>, accessed November 2009
- [18] PERKINS C.E., BELDING-ROYER E.M., DAS S.R.: 'Ad hoc on-demand distance vector (AODV) routing. mobile ad hoc'. Internet Engineering Task Force (IETF) INTERNET-DRAFT <draft-ietf-manet-aodv-13.txt>, <http://tools.ietf.org/html/draft-ietf-manet-aodv-13>, accessed November 2009
- [19] ALLMAN M., PAXSON V., STEVENS W.: 'TCP congestion control'. Internet Engineering Task Force (IETF) INTERNET-DRAFT, <http://www.ietf.org/rfc/rfc2581.txt>, accessed November 2009
- [20] YAN L., XINHENG W., CAIXING L.: 'Scalable video streaming in wireless mesh networks for education'. Proc. IEEE Int. Symp. on IT in Medicine & Education (ITME2009), Jinan, China, 2009, pp. 840-845
- [21] XUE Q., GANZA A.: 'Ad hoc QoS on-demand routing (AQOR) in mobile ad hoc networks', *J. Parallel Distrib. Comput.*, 2003, **63**, (2), pp. 154-165
- [22] HU S.: 'Multicast routing protocols in mobile ad hoc networks', PhD thesis, North Carolina State University, Raleigh, North Carolina, USA, 2008
- [23] DARESHOORZADEH A., DEGHAN M., MOTLAGH M.R.: 'Quality of service support for ODMRP multicast routing in ad hoc networks'. Proc. Sixth Int. Conf. ADHOC-NOW, Morelia, Mexico, September 2007, pp. 237-247
- [24] Network Simulator-2: <http://www.isi.edu/nsnam/ns/>, accessed November 2009
- [25] MAODV NS2 Implementation By Thomas Kunz at Carleton University Canada: <http://www.sce.carleton.ca/wmc/code.html>, accessed November 2009

Copyright of IET Communications is the property of Institution of Engineering & Technology and its content may not be copied or emailed to multiple sites or posted to a listserv without the copyright holder's express written permission. However, users may print, download, or email articles for individual use.